

Numerical Investigation into Velocity and Temperature Fields Over Smooth and Rough Ducts for Several Types of Turbulators

Dr. Sabah Tarik Ahmed¹ Dr. Waheed S. Mohammed* & Laith J.H.* Received on: 1/3/2006

Accepted on: 12/7/2006

Abstract

Numerical study on a laminar and turbulent fluid flow and temperature distribution in a rectangular duct with six types of vortex generators has been carried out. A modified version of ESCEAT three-dimension code has been used to solve Navier-Stokes and energy equations. The effect of vortex generator type, geometrical configuration, and dimensions on flow and temperature in different planes has been presented. The purpose of the present investigation is to highlight the complex three-dimensional interaction of the vortices generated by wings and other vortex generators to understand how such vortices configurations structure the velocity and temperature fields. Experiment in terms of velocities and temperatures vectors and contours were performed on 6 configurations, which experiments are (fin, fence, rib, wing-type, rectangular-type, and winglet-type) vortex generators. The results show good agreement with published data.

Keywords: Vortex Generator, Three-Dimensional flow, Wall function, Laminar and Turbulent.

الخلاصة

تم إجراء دراسة عددية على توزيع الجريان ودرجة الحرارة للمائع لحالتي الجريان الطبقي والاضطرابي داخل قنوات مستطيلة حاوية على ستة أنواع من مولدات الدوامات. واستخدم لذلك نسخة مطورة من برنامج (ESCEAT) بثلاثة أبعاد لحل معادلتين نافيير-ستوكس والطاقة. حيث تم دراسة تأثير نوع مولد الدوامات وشكله الهندسي وأبعاده على الجريان ودرجة الحرارة في مختلف المستويات. ان الغرض من البحث الحالي هو لتسليط الضوء على التأثير المعقد ذو الثلاثة أبعاد للدوامات المتولدة بواسطة الجَنِيحات (wings) ومولدات الدوامات الأخرى لفهم كيف ان الأشكال الهندسية لهذه الدوامات تُشكل مجالي السرعة ودرجة الحرارة. لقد أخذت النتائج بصيغة متجهات وكنتورات (منحنيات مقلقة) للسرعة ودرجات الحرارة لستة أشكال من مولدات الدوامة وهي الزعنفة (fin) والحاجز (fence) والنتوء (rib) وجَنِيح (wing) وعائق مستطيل (rectangular) وعائق نوع (winglet). وقد أثبتت النتائج توافقاً وتطابق جيد مع تلك المنشورة سابقاً.

Nomenclature

			Greek Symbol
B	Width of the duct		
Br	ratio of wing span to width of the duct, b/B	α	Inclination angle
b	width of the VG (wing span)	β	Angle of attack

* Mech. Eng. Dept., University of Technology, Baghdad, IRAQ.

C_1, C_2, C_D	coefficient in turbulence models, =1.43, 1.92, 0.09 respectively	β_1	thermal expansion coefficient
C_p	specific heat	γ	aspect ratio of the duct , B/H
e	VG thickness	δ	aspect ratio of the wing , 2b/l
g	gravitational acceleration	Γ	diffusion coefficient = μ / σ
G_B	buoyancy production	ε	energy dissipation
G_K	generation rate of turbulence energy	μ	dynamic viscosity
H	duct height	ρ	fluid density
h	VG height	σ	prandtl number
hd	hydraulic diameter		Subscript
k	turbulent kinetic energy	k, ε	refer to turbulence model equation
L	duct length	in	iInlet condition
l	VG length or chord	ref	reference condition
p	pressure	t	turbulent
s	distance between winglet-pair (narrow side)	wall	condition at wall
S_T	source term	x,y,z	refer to cartesian coordinates
q_w	wall heat flux		Superscript
T	temperature	+	dimensionless value
U, V, W	mean velocity components	'	fluctuations relative to the time-averaged values
u, v, w	component of Velocity vector in x,y, and z direction	—	time-average values of products of fluctuating quantities
x, y, z	Physical or Cartesian coordinates		Abbreviation
		ESCE	elliptic equation solver for convection and Heat Transfer
		AT	
		k- ε	two-equations turbulence model
		PDES	partial differential equations
		SIMP	semi-Implicit Method for pressure Linked Equation
		LE	
		VG	vortex Generator

Introduction

Configurations involving arrangements of sequential baffles (ribs, thin obstacles etc.) attached to a wall are commonly used for supporting and mixing purposes in heat exchangers, nuclear reactors cores, air-cooled solar collectors, some electronic circuit boards, internally cooled turbine blades, wastewater aeration tanks as well as chemical mixers and other chemical engineering applications. In some situations, turbulence generation and mixing associated with separation are desirable whereas in others separation is to be avoided as it causes a pressure loss [1]. Turbulence promoters or roughness elements have been used to improve the heat transfer. These roughness elements have been set on a heat transfer surface. The mechanism augmented heat transfer is complicated since the effects of the extended surface and turbulence generation are combined [2]. The character of the surface of the walls which makes up a duct strongly influence fluid flows along the ducts. Consequently, it would be more difficult to predict the characteristics of the flow and of the heat transfer in noncircular ducts with rough surfaces [3]. The basic idea of the heat transfer augmentation is not only to disturb the velocity temperature profiles close to the walls, but also to create a secondary flow that will exchange heat and momentum between the wall regions and the core region [4].

There are multi-types of these turbulators or vortex generators, Fig.1 shows only six types that are used in this work.

Longitudinal vortices generated by wings at an angle of attack spiral the flow around their axes and persist to

hundreds of wing chords downstream of the wing. When longitudinal vortex generators are placed near a heat transfer surface or when they are part of the heat transfer surface, they increase the heat transfer by transporting fluid from the wall in to the free stream and vice versa. Essential for the effectiveness of a vortex generator in substantially enhancing the heat transfer over a large area is the vortex strength that can be generated per unit area of the vortex generator. From theory and experiment it is well known that slender delta wings are the most effective longitudinal vortex generators, Fig. 1-a, [5].

The purpose of this paper is to present numerical model for the velocity and temperature fields over a smooth and six type VGs roughened surfaces.

Vortex generators by means of delta wing and winglet-type and by rectangular winglet-type have been previously observed by [5 & 6]. They have studied laminar velocity and temperature fields with a row of built-in VGs with a range of Reynolds number. The experiment results and the analytical methods show a heat transfer enhancement because of the longitudinal vortices that are deformed. Also, the delta wing shows by far the best performance of all configurations. The increase in friction factor appears to be proportional to the projected cross flow area for all geometries.

Fluid flow and heat transfer over a transverse ribbed surface in a rectangular channels were carried out by [7&8]. The computational and experimental studies undertake the effect of the channel aspect ratio on the distribution of the local heat

transfer coefficient in rectangular channels for a range of Reynolds number, channel width-to-height ratio and rib spacing. There is good agreement between prediction and measurements. Based on the law of the wall similarity and the application of the heat-momentum analogy, a general correlation of friction factor and heat transfer was developed.

The turbulent flow over a well-defined rough surfaces, walls, and elements numerically and experimentally is presented by [2 , 3 & 9]. The researchers studied momentum - and heat - transfer characteristics.

Works about heat transfer enhancement by using transverse and pin fins have been investigated by [10 & 11]. A numerical study was done on laminar fluid flow and forced convection heat transfer within horizontal channels to which one or two pairs of transverse fins are attached for different Reynolds numbers and various geometric arrangements. Experiments have been conducted to study the turbulent heat transfer and friction characteristics in pin fin channels.

Measurements and computations of the mean stream wise velocity and its fluctuation for an arrangement of two similarly fences mounted in tandem in fully developed channel flow have been reported by [1].

Mathematical and numerical Formulation

The mathematical formulation of fluid flow problems is governed by basic conservation principles namely the conservation of mass, momentum and energy. These principles can be expressed in terms of (PDES) for both laminar and turbulent flow regimes.

The numerical modeling of fluid flow is of a great significance in all applications. Finite volume method offers a great simplicity to numerical solution of partial, non-linear differential equations in Cartesian coordinate system [12 – 14].

General Conservation Equations

- (i) Mass conservation (continuity)

For steady incompressible, three-dimensional flows, for laminar flow:

$$\frac{\partial U}{\partial x} + \frac{\partial V}{\partial y} + \frac{\partial W}{\partial z} = 0 \dots\dots\dots (1)$$

and for turbulent flow, equation (1) is replaced by the sum of a time-mean component and a fluctuating component i.e.;

$$U = u + u', V = v + v', W = w + w'$$

then, the mass conservation equation becomes;

$$\frac{\partial u}{\partial x} + \frac{\partial v}{\partial y} + \frac{\partial w}{\partial z} = 0 \dots\dots\dots (2)$$

Since the fluctuating in $u', v',$ and w' occurs over a short time interval so that $u \approx U, v \approx V,$ and $w \approx W$.

(ii) Conservation of momentum
(for turbulent flow)

X-direction (U momentum):

$$\begin{aligned} \frac{\partial}{\partial x}(u) + \frac{\partial}{\partial y}(v) + \frac{\partial}{\partial z}(w) &= -\frac{1}{r} \cdot \frac{\partial p}{\partial x} + \frac{1}{3} \cdot \\ \frac{1}{r} \cdot \frac{\partial}{\partial x}(\mu \cdot \nabla N) + \frac{1}{r} \cdot \nabla^2 \mu u + g_x + \frac{\partial}{\partial x}(\overline{-u'u'}) & \\ + \frac{\partial}{\partial y}(\overline{-u'v'}) + \frac{\partial}{\partial z}(\overline{-u'w'}) \dots \dots \dots (3) \end{aligned}$$

where: $\nabla N = \frac{\partial U}{\partial x} + \frac{\partial V}{\partial y} + \frac{\partial W}{\partial z}$ &

$$\nabla^2 = \frac{\partial}{\partial x} \left(\frac{\partial}{\partial x} \right) + \frac{\partial}{\partial y} \left(\frac{\partial}{\partial y} \right) + \frac{\partial}{\partial z} \left(\frac{\partial}{\partial z} \right)$$

Y-direction (V momentum):

$$\begin{aligned} \frac{\partial}{\partial x}(u) + \frac{\partial}{\partial y}(v) + \frac{\partial}{\partial z}(w) &= -\frac{1}{r} \cdot \frac{\partial p}{\partial y} + \\ \frac{1}{3} \cdot \frac{1}{r} \cdot \frac{\partial}{\partial y}(\mu \cdot \nabla N) + \frac{1}{r} \cdot \nabla^2 \mu v + g_y + & \\ \frac{\partial}{\partial x}(\overline{-u'v'}) + \frac{\partial}{\partial y}(\overline{-v'v'}) + \frac{\partial}{\partial z}(\overline{-v'w'}) \dots \dots (4) \end{aligned}$$

Z-direction (W Momentum):

$$\begin{aligned} \frac{\partial}{\partial x}(u) + \frac{\partial}{\partial y}(v) + \frac{\partial}{\partial z}(w) &= -\frac{1}{r} \cdot \frac{\partial p}{\partial z} + \\ \frac{1}{3} \cdot \frac{1}{r} \cdot \frac{\partial}{\partial z}(\mu \cdot \nabla N) + \frac{1}{r} \cdot \nabla^2 \mu w + g_z + & \\ \frac{\partial}{\partial x}(\overline{-u'w'}) + \frac{\partial}{\partial y}(\overline{-v'w'}) + \frac{\partial}{\partial z}(\overline{-w'w'}) \dots \dots (5) \end{aligned}$$

and for laminar flow, the last three terms in equations (3),(4),and (5) do not exist and are replaced $u, v, \text{ and } w$ by $U, V, \text{ and } W$, assuming a similar

expression for the pressure P (i.e. $P = p + p'$).

(iii) Conservation of thermal energy (for turbulent flow)

$$\begin{aligned} \frac{\partial}{\partial x}(\Gamma \cdot \frac{\partial T}{\partial x}) + \frac{\partial}{\partial y}(\Gamma \cdot \frac{\partial T}{\partial y}) + \frac{\partial}{\partial z}(\Gamma \cdot \frac{\partial T}{\partial z}) + \\ \frac{\partial}{\partial x}(-\rho \cdot \overline{u'T'}) + \frac{\partial}{\partial y}(-\rho \cdot \overline{v'T'}) + \frac{\partial}{\partial z}(-\rho \cdot \overline{w'T'}) \\ + S_T = 0 \dots \dots \dots (6) \end{aligned}$$

And for turbulence models:

$$\begin{aligned} (\overline{u'^2} = \overline{v'^2} = \overline{w'^2}) \text{ and:} \\ \left. \begin{aligned} -\rho \cdot \overline{u'u'} &= 2 \cdot \mu_t \frac{\partial u}{\partial x} - \frac{2}{3} \rho k \\ -\rho \cdot \overline{v'v'} &= 2 \cdot \mu_t \frac{\partial v}{\partial y} - \frac{2}{3} \rho k \\ -\rho \cdot \overline{w'w'} &= 2 \cdot \mu_t \frac{\partial w}{\partial z} - \frac{2}{3} \rho k \\ -\rho \cdot \overline{u'v'} &= \mu_t \left(\frac{\partial u}{\partial y} + \frac{\partial v}{\partial x} \right) \\ -\rho \cdot \overline{v'w'} &= \mu_t \left(\frac{\partial v}{\partial z} + \frac{\partial w}{\partial y} \right) \\ -\rho \cdot \overline{u'w'} &= \mu_t \left(\frac{\partial u}{\partial z} + \frac{\partial w}{\partial x} \right) \end{aligned} \right\} \dots (7) \end{aligned}$$

where:

$$k = \frac{1}{2} \left[(\overline{u'})^2 + (\overline{v'})^2 + (\overline{w'})^2 \right]$$

and for laminar flow, the fourth, fifth, and sixth terms in equation (6) do not exist, and are again written $\tilde{T} = T + T'$, where T is the time-mean temperature and T' is the fluctuating from mean.

The $k - \varepsilon$ Turbulence Model

Two-equation turbulence model will be more appropriate for elliptic equation, such as the present case flows. For such flows a two-equation turbulence model ($k - \varepsilon$) has been adopted for the present work.

The transport equations for k and ε are as follow:

$$\frac{\partial}{\partial x}(\Gamma_k \frac{\partial k}{\partial x}) + \frac{\partial}{\partial y}(\Gamma_k \frac{\partial k}{\partial y}) + \frac{\partial}{\partial z}(\Gamma_k \frac{\partial k}{\partial z}) + G_k - \rho \cdot \varepsilon + G_B = 0 \dots (8)$$

where:

$$G_k = \mu_t \left\{ 2 \left[\left(\frac{\partial u}{\partial x} \right)^2 + \left(\frac{\partial v}{\partial y} \right)^2 + \left(\frac{\partial w}{\partial z} \right)^2 \right] + \left(\frac{\partial u}{\partial y} + \frac{\partial v}{\partial x} \right)^2 + \left(\frac{\partial u}{\partial z} + \frac{\partial w}{\partial x} \right)^2 + \left(\frac{\partial v}{\partial z} + \frac{\partial w}{\partial y} \right)^2 \right\}$$

$$G_B = -\beta_1 g \frac{\mu_t}{\sigma_t} \cdot \frac{\partial T}{\partial y} ,$$

$$\mu_t = C_D \cdot \rho \cdot k^2 / \varepsilon$$

$$\frac{\partial}{\partial x}(\Gamma_\varepsilon \frac{\partial \varepsilon}{\partial x}) + \frac{\partial}{\partial y}(\Gamma_\varepsilon \frac{\partial \varepsilon}{\partial y}) + \frac{\partial}{\partial z}(\Gamma_\varepsilon \frac{\partial \varepsilon}{\partial z}) + \frac{\varepsilon}{k} [C_1 \cdot G_k - C_2 \cdot \rho \varepsilon] = 0 \dots (9)$$

Wall function and heat flux

It should be mentioned that the heat flux across the viscous sub-layer is

assumed to be constant. As in momentum transport treatment, the point $Y^+=11.5$ is also defined here for disposing buffer layer. For $Y^+ \leq 11.5$ the transport is assumed to be due to molecular activity and the expression for the heat flux parameter T^+ is a simple one.

For $Y^+ \geq 11.5$ where

$$\frac{\Gamma_t}{\Gamma} \gg 1, q \approx q_{wall} \text{ calculate}$$

q_{wall} from the following relation:

$$T^+ = \frac{(T_{wall} - T_p) \rho C_p u_t}{q_{wall}} = \sigma_t \left[u^+ + P \left(\frac{\sigma}{\sigma_t} \right) \right] \dots (10)$$

$$\frac{q_{wall}}{C_p} = \frac{\rho u_t (T_{wall} - T_p)}{\sigma_t \left[u^+ + P \left(\frac{\sigma}{\sigma_t} \right) \right]} \dots (11)$$

$$P \left(\frac{\sigma}{\sigma_t} \right) = \frac{9.0 \left[\left(\frac{\sigma}{\sigma_t} \right) - 1.0 \right]}{\left[\frac{\sigma}{\sigma_t} \right]^{1/4}} \dots (12)$$

Conditions

- A. Initial $u=v=0$, $w=w_{in}$, $k=k_{in}=0.00135 * (w_{in})^2$, $\varepsilon = \varepsilon_{in}=0.09 * (k_{in})^{1.5} / (0.03 * hd)$, $T=T_{ref}$
- B. At inlet $u=v=0$, $w=w_{in}$, $k=k_{in}$, $\varepsilon = \varepsilon_{in}$, $\mu=\mu_{ref}$, $T=T_{in}$
- C. At walls and VGs surfaces $u=v=w=k=\varepsilon=0$, $\mu = \mu_{ref}$, $T=T_{wall}$

D. At exit all variables equal to the same variables just before one plane.

The SIMPLE procedure that uses a staggered grid use a power-law differencing scheme with finite volume method to solve the (u , v , w , p , k , ϵ) equations.

Results and Discussion

A large number of computations have been performed at different VG

types, Reynolds numbers, ducts and VGs configurations and dimensions, which will be discussed below.

An important step in our code development is to validate its results using published data from other sources.

Fig. (2) shows a comparison of the computational result of Sabah [14], with the present result for laminar flow in a smooth duct for grid size (20x17x28). The results show a good agreement.

Fig. (3) shows another comparison of a computational result of Biswas et al. [15], for laminar flow in a channel with built-in wing-type VG for grid size (26x15x60) and channel's dimensions (0.4x0.2x1.68) m³ and wing dimensions ($h=0.156$ m, $l=0.316$ m, $b=0.15$ m). The figure shows the first half of the channel length. Again the comparison appears to be fairly good.

As can be seen from fig.(2) & (3), the present code gives an acceptable simulation for both cases, i.e., the simplest one which is for smooth duct without turbulator and the more complex case, i.e., the rough duct with wing-type VG. Therefore, the present code could be used to handle

other complicated flows using several VG configurations as shown in fig. (1). One of such VG configurations is presented in fig. (4) which shows a finned duct (0.5x0.15x0.75) m³ with grid size (21x17x29) with $l=0.26$ m ($x=0.12-0.38$) m and $h=0.03$ m. The obtained heat and flow pattern for this finned duct are presented in this figure. The presence of fins causes the flow to detach from the wall surface so that recirculation occurs in the rear of each fin. Owing to the vortex motion, temperature of recirculation

flows becomes rather high for perfectly conductive fins.

Airflow and isothermal contours in a fenced duct configuration are shown in Fig. (5). The related dimensions are the same with the finned duct but with different height fences ($e=27$ mm, $h=28$ & 56 mm and $l=0.5$ m), the shorter one placed at $z=0.24$ m and the other at $z=0.515$ m. The inlet temperature was $16C^{\circ}$ and the wall and fences surfaces at $40C^{\circ}$. It can be seen, how the VGs distribute the temperature and then enhance heat transfer.

The effect of ribs and its locations are presented in Fig. (6-a to 6-d). Fig. (6-a) gave the velocity vectors for staggered ribbed duct (0.16x0.08x0.6) m³ and (10x19x60) grid size and ($l=0.16$ m, $e=10$ mm, and $h=13$ mm), for laminar case at $Re=2119$. It shows a recirculation flows near the upper surface. Fig. (6-b) shows the flow at two-ribbed duct placed at the lower surface with the same duct dimensions and (19x15x31) grid size and ($l=0.16$, $e=20$ mm, and $h=17$ mm), and $Re=2119$. The developing

flow in the entrance region is clear in the figure. The turbulent flow ($Re=6293$) is tackled in figure (6-c & 6-d), where Fig. (6-c) highlighted the velocity image (w/w_{in}) for staggered configuration for the same duct and ($11 \times 21 \times 31$) grid size. The dark color shows the small values of the velocity lie behind the ribs due to the vortex generated at that location. The temperature distributions, (T/T_{wall}) are given in fig. (6-d) with staggered configuration and $T_{in}=7C^{\circ}$ and $T_{wall}=27C^{\circ}$. The effect of the previously maintained flow vortices on temperature gradient is very clear in this figure.

For slender delta wings in a free stream, fig. (7, 8) show the vortex and flow structure and temperature distributions. Fig. (7-a & 7-b) represents the laminar case of the wing. Since Fig.(7-a) represents velocity contour for v -velocity component at $Re=500$, the symmetry of the flow is very clear in this figure. This location is very close to the beginning of the wing. Fig. (7-b) shows the isotherms for thermally and hydro dynamically developing duct flows with a built-in delta wing. It can be seen that the variation of temperature before the wing is very large while the temperature values after the wing is approximately constant. The turbulent behavior is presented in Fig. (7-c & 7-d). Fig. (7-c) shows the velocity along the duct at $Re=153846$, while Fig. (7-d) shows temperature field, the vortex generator disturbs the temperature field strongly. The difference in temperature field between laminar

case and the turbulent one is large as can be in for Fig. (7-b & 7-d). Near the top wall, then, appears a small temperature gradient above and behind the wing, which was not in the laminar case. And Fig. (7-e & 7-f) shows a comparison between the laminar and turbulent temperature distributions at the given location. The difference is quite clear between the two figures, which can be attributed to the turbulent effect (vortices). Fig. (7-e) shows temperature contours in cross section for laminar flow with delta wing geometries as in Fig. (3), while Fig. (7-f) is for turbulent flow. In the wing tip region the vortices suck low-velocity fluid into the vortex and bring it close to the wing, which leads to a thickening of the temperature

boundary downstream of the wing base.

Fig. (8) shows the formation of vortex pair for delta wing previously given in Fig. (3). The leading edge vortices have a circular structure and disappear gradually up to the end of the duct.

Fig. (9) shows velocity vectors and temperature contours for duct flow with winglet pair ($0.5 \times 0.15 \times 0.75$) m^3 duct with ($21 \times 17 \times 29$) grid size. Winglet dimensions are: $l=55$ mm, $h=19$ mm, and $a = 43.7^{\circ}$, and the two winglets are from $z=0.23$ m to $z=0.29$ m. Fig. (9-a & 9-b) gives, the laminar case of $Re=1538$. Fig. (9-a) shows cross flow at $Z=0.4$ m, it shows two vortices at the same direction. And Fig. (9-b) shows cross-temperature contours at $z=0.26$ m. Fig. (9-c & 9-d) gives the turbulent counter part of the case at $Re=153846$. Fig. (9-c) shows

cross flow at $z=0.75$ m. Two small vortices inside a big one appear in the figure, the small vortices shift to the direction of rotation. Fig. (9-d) shows the temperature distribution at $z=0.26$ m too. The differences between the temperature contours of Fig. (9-b) & (9-d) can explain the theory of force convection, i.e., the convection of heat is large for small velocities and vice versa.

Finally, fig. (10) describes the simulation of laminar and turbulent flow and heat for rectangular wing in a duct similar to that of Fig. (9) for the Re & temperature field. The VG dimensions are: $l=55$ mm, $h=19$ mm and $b = 19.1^\circ$, also from $z=0.23$ m to $z=0.29$ m. Fig. (10-a) shows u-velocity component contours at $z=0.24$ m for the laminar flow. Symmetrical values appear clearly in the figure. Fig. (10-b) represents

temperature contours at midplane for laminar flow. Fig. (10-c) shows v-velocity component contours at $z=0.24$ m for turbulent flow, and Fig. (10-d) represents temperature contours at midplane for turbulent flow.

Concluding Remarks

Based on the results presented and discussed, the main conclusions are:

- 1- Numerical study was carried out to predict the velocities and temperatures for laminar and turbulent forced convection flows in internally roughened rectangular ducts. Six types of turbulators are used. The flow is characterized by recirculation zones and significant flow distortion.

- 2- The study includes the prediction of the presence of two-finned duct on the bottom surface of a duct. These fins interrupt the development of boundary layers, and hence exhibit great influence on the local flow behavior.

- 3- The ribbed-rough ducts also predicted the influence on the secondary flow. This gives a peculiarity in the contours map which is similar to that observed in the contours of the mean velocity.

- 4- The study on the delta-wing's effect shows the generation of a pair of counterrotating longitudinal vortices along their leading edges that diverge slightly depending on the aspect ratio of the wing. The longitudinal vortices follow somewhat the wing inclination until they are redirected by the duct walls.

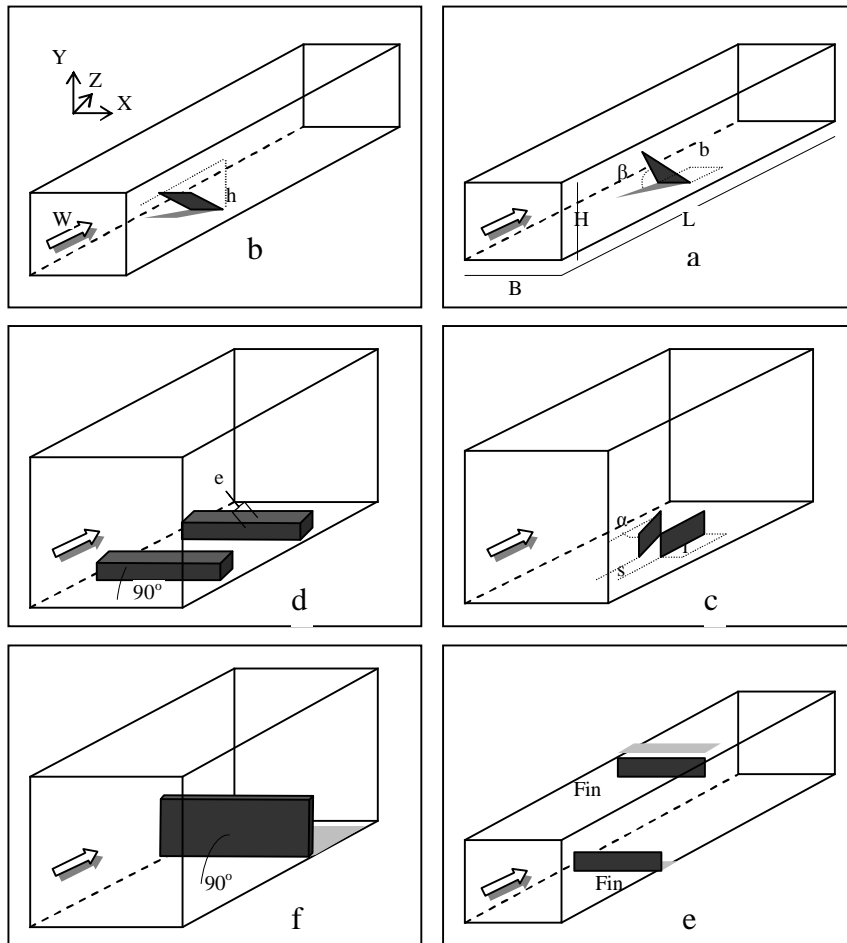


Fig.(1) Some types of Vortex Generators (VGs) (the figures not to scale): a) Delta wing, b) Rectangular wing, c) Winglet, d) Rib, e) Fin, and f) Fence.

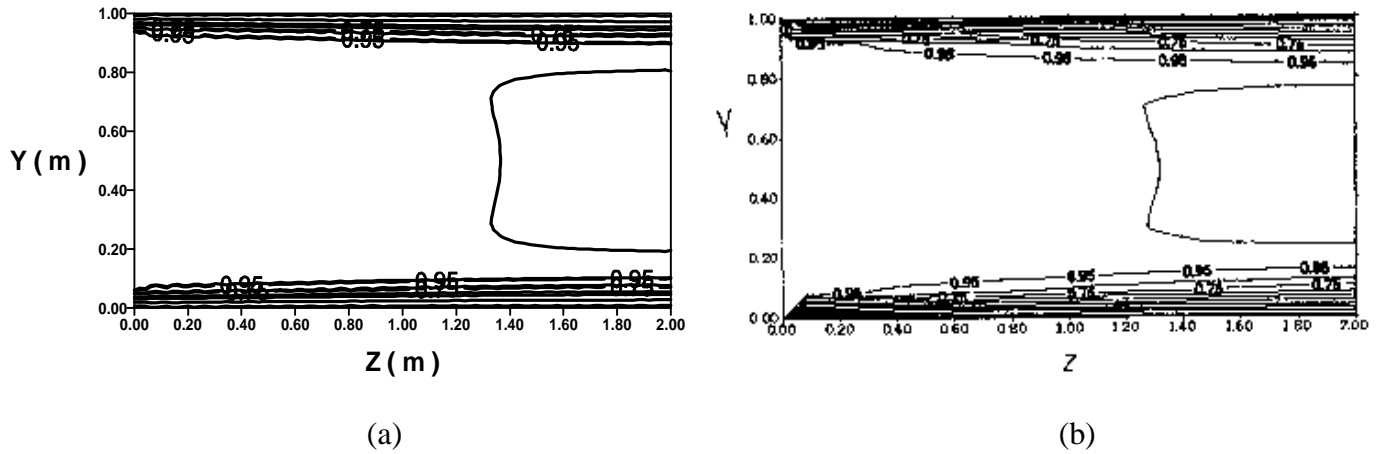


Fig.(2) Variation in (w/w_{in}) at mid plane and $Re=500$ (a) Present result (b) Result of [14].

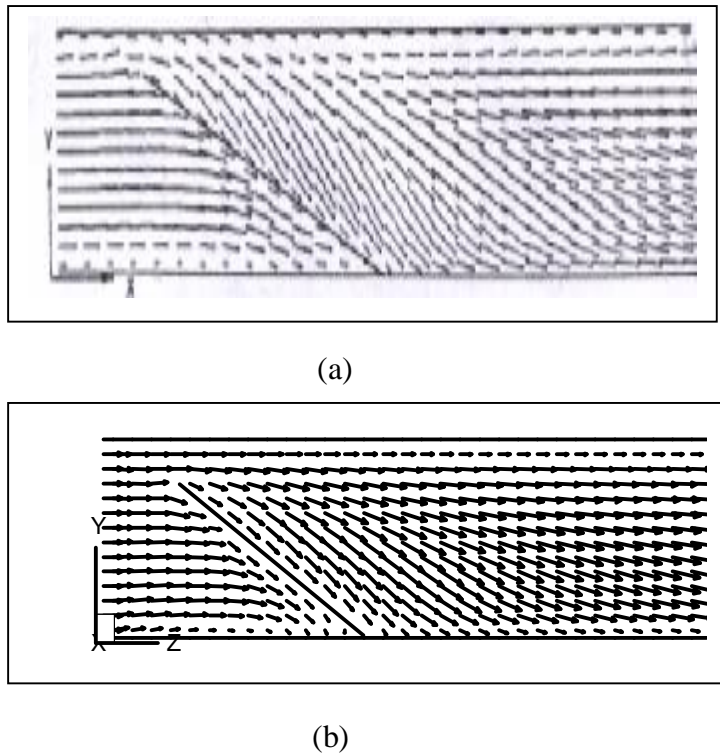


Fig.(3) Longitudinal velocity vectors at mid plane and $Re=500$ with $\sigma = 0.7$, $Br=0.375$, $\delta=1$, $\gamma=2$, $\beta=2^\circ$, x (or z in present result) = 0.0 - 0.84 m (a) Present result (b) Result of [15].

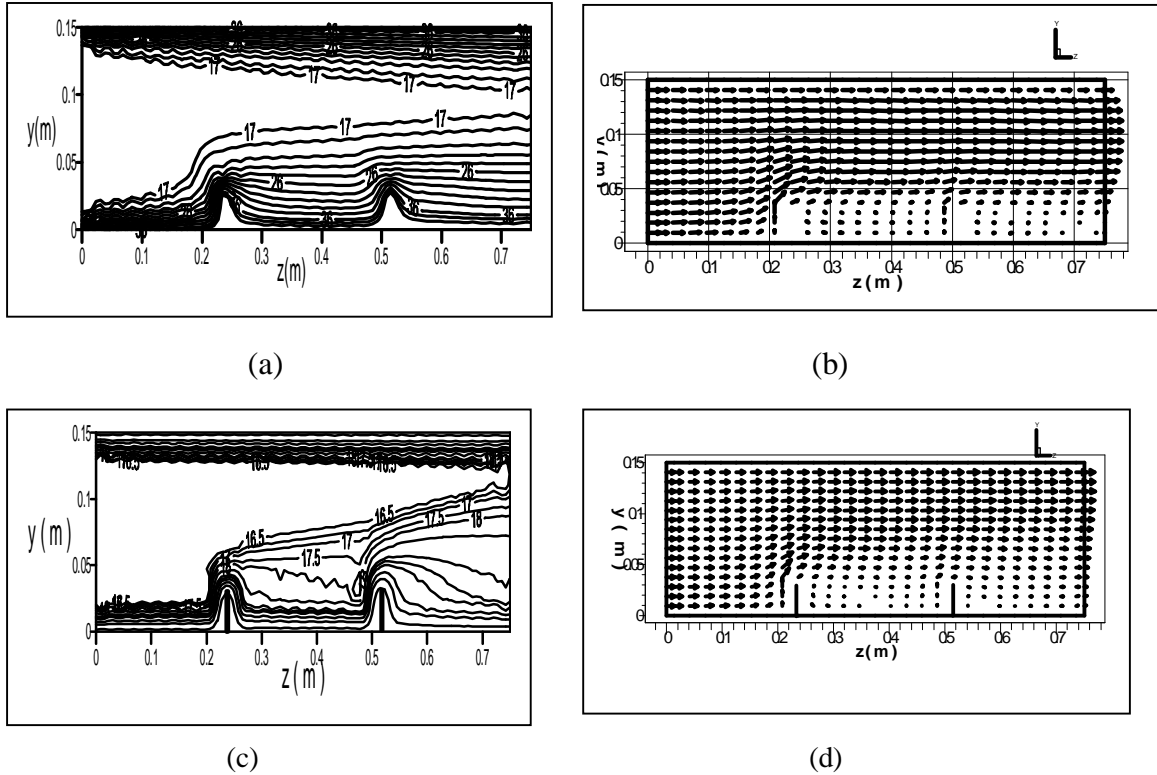
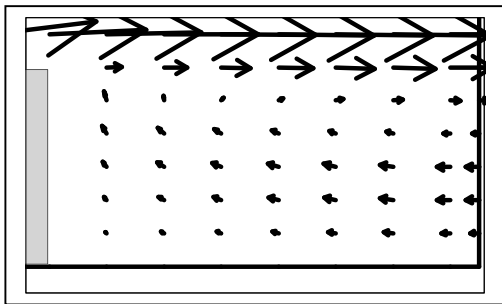
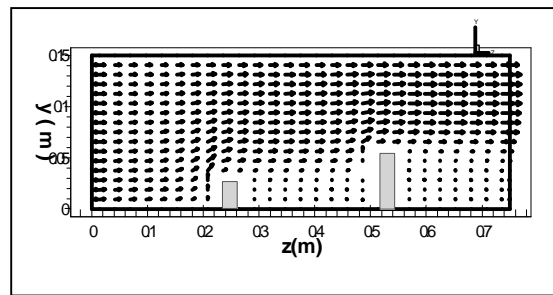


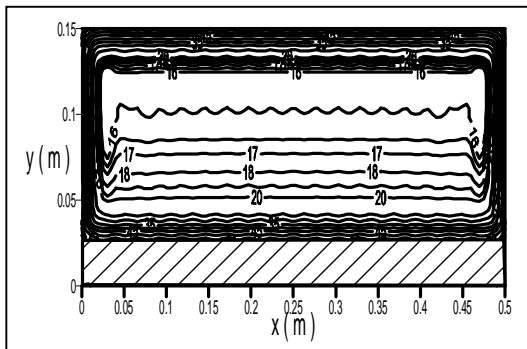
Fig.(4) Variation in isothermal contour and flow field at mid plane for laminar and turbulent flows At $Re=1538$: (a) Isothermal contour $T_{in}=16\text{ C}^\circ$ & $T_w=40\text{ C}^\circ$, (b) Velocity vector. At $Re=135846$: (c) Isothermal contour $T_{in}=16\text{ C}^\circ$ & $T_w=40\text{ C}^\circ$, and (d) Velocity vector.



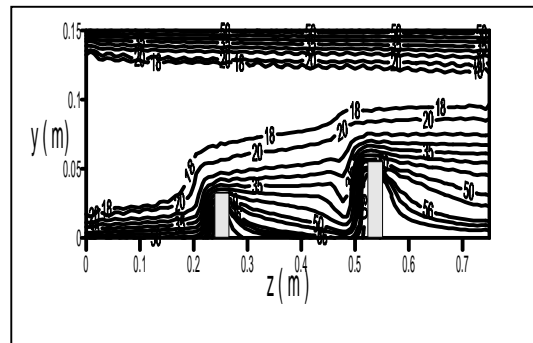
(a)



(b)

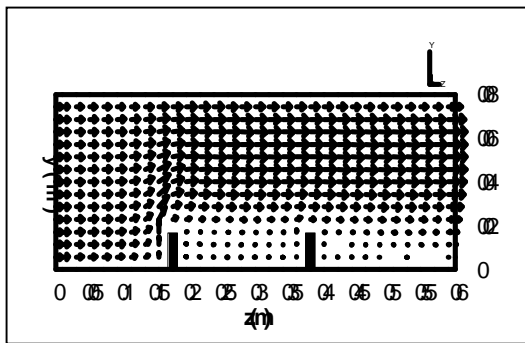


(c)

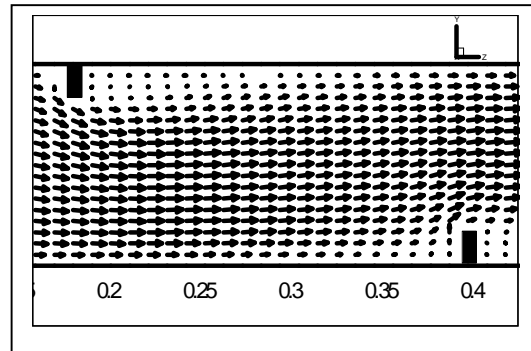


(d)

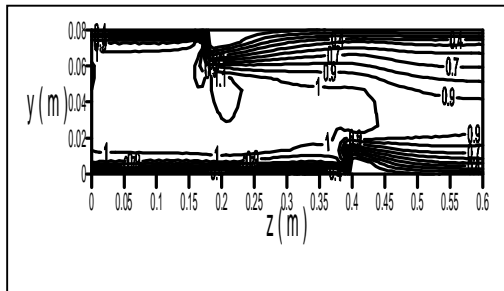
Fig.(5) Velocity vectors and temperature contours at $Re=1538$: (a) Close view , (b) Velocity vector at mid plane , (c) Temperature contours at cross section ($z=0.23$)m and (d) Temperature contours at mid plane.



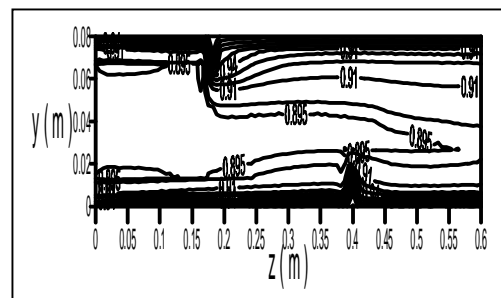
(a)



(b)



(c)



(d)

Fig.(6) Velocity vectors and temperature contours for : (a) Staggered ribs ($z=0.18$ m & $z=0.4$ m) at $x=66$ mm for laminar flow, (b) Two ribs ($z=0.19$ m & $z=0.39$ m) for laminar flow, (c) (w/w_{in}) at mid plane for turbulent flow , and (d) (T/T_{wall}) at mid plane for turbulent flow .

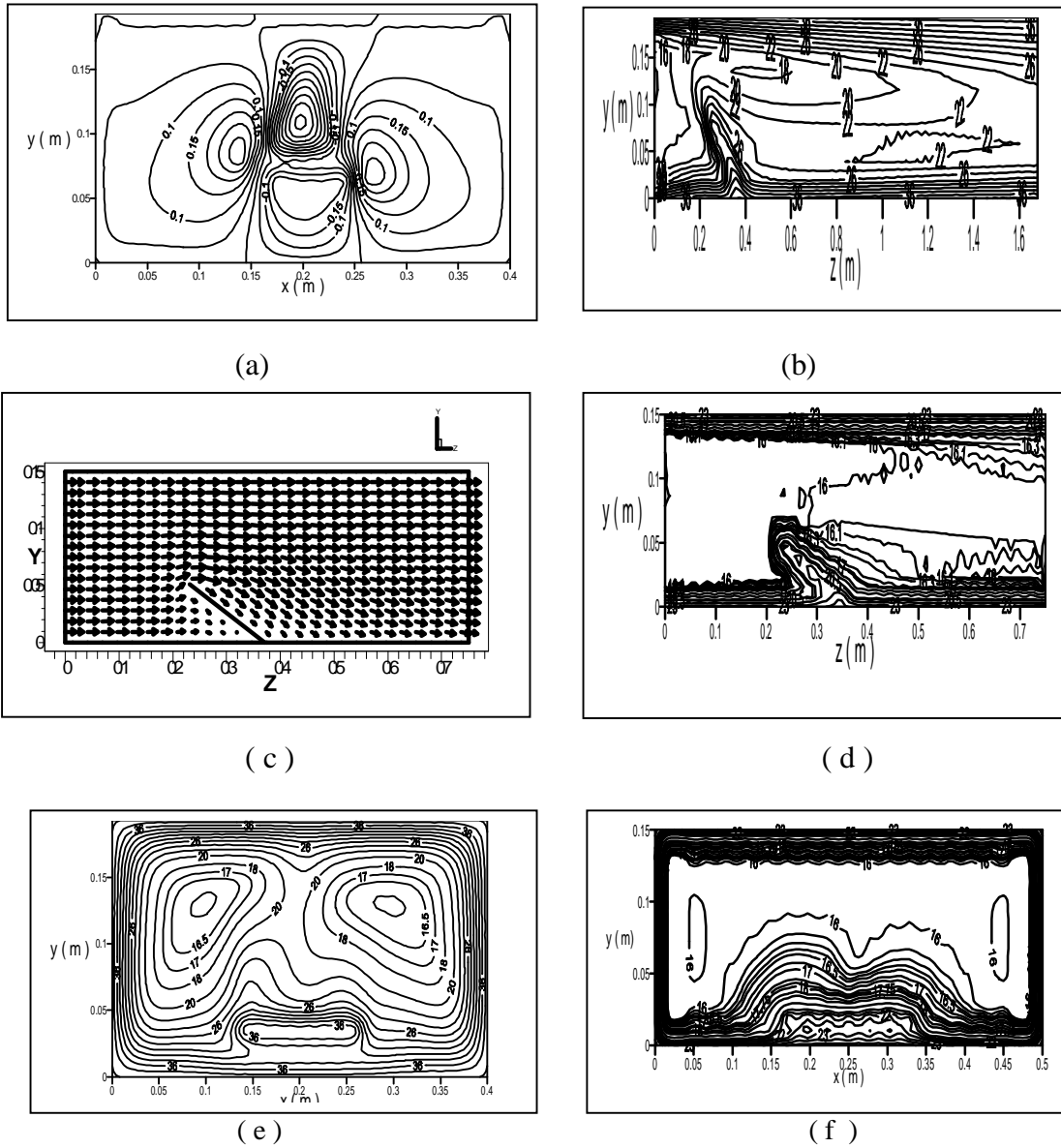


Fig.(7) Flow and temperature distirbution for wing-type VG :
 (a) (v/w_{in}) at $z=0.24$ m for $(0.4 \times 0.2 \times 1.68)$ m³ duct with $(26 \times 15 \times 60)$ grid size in $(x-y)$ plane for laminar flow, (b) T at $x=0.16$ m in $(y-z)$ plane for laminar flow,
 (c) w at mid $(y-z)$ plane for $(0.5 \times 0.15 \times 0.75)$ m³ duct with $(21 \times 17 \times 29)$ grid size for turbulent flow, (d) T at mid $(y-z)$ plane for turbulent flow, (e) T at $z=0.33$ m while $(T_{wall}=40C^{\circ} \& T_{in}=16C^{\circ})$ in $(x-y)$ plane for laminar flow, and (f) T at $z=0.31$ m with wing properties : $\sigma =0.7$, $Br=0.5$, $\delta=3.7$, $\gamma=3.3$, $\beta=19.3^{\circ}$ (wing tip at $z=0.23$ m and wing base at $z=0.37$ m) while $(T_{wall}=25C^{\circ} \& T_{in}=16C^{\circ})$ in $(x-y)$ plane for turbulent flow.

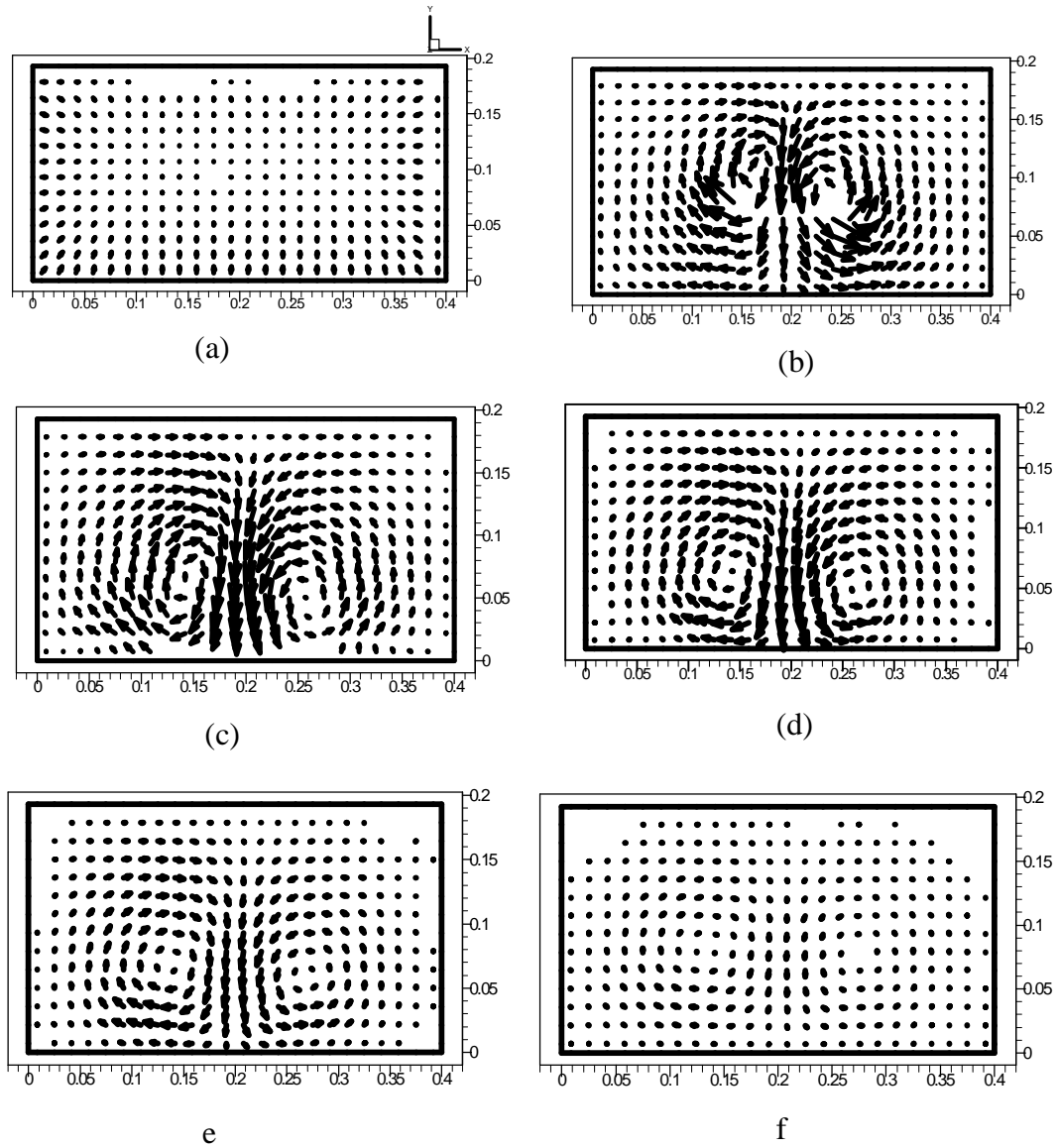


Fig.(8) The development of the cross flow for wing-type VG in (x-y) plane for laminar flow and wing dimensions ($h=0.156$ m, $l=0.316$ m, $b=0.15$ m) while (wing tip at $z=0.1$ m and wing base at $z=0.42$ m) at : (a) $z=0.04$ m , (b) $z=0.24$ m , (c) $z=0.39$ m , (d) $z=0.53$ m , (e) $z=0.82$ m , and (f) $z=1.68$ m.

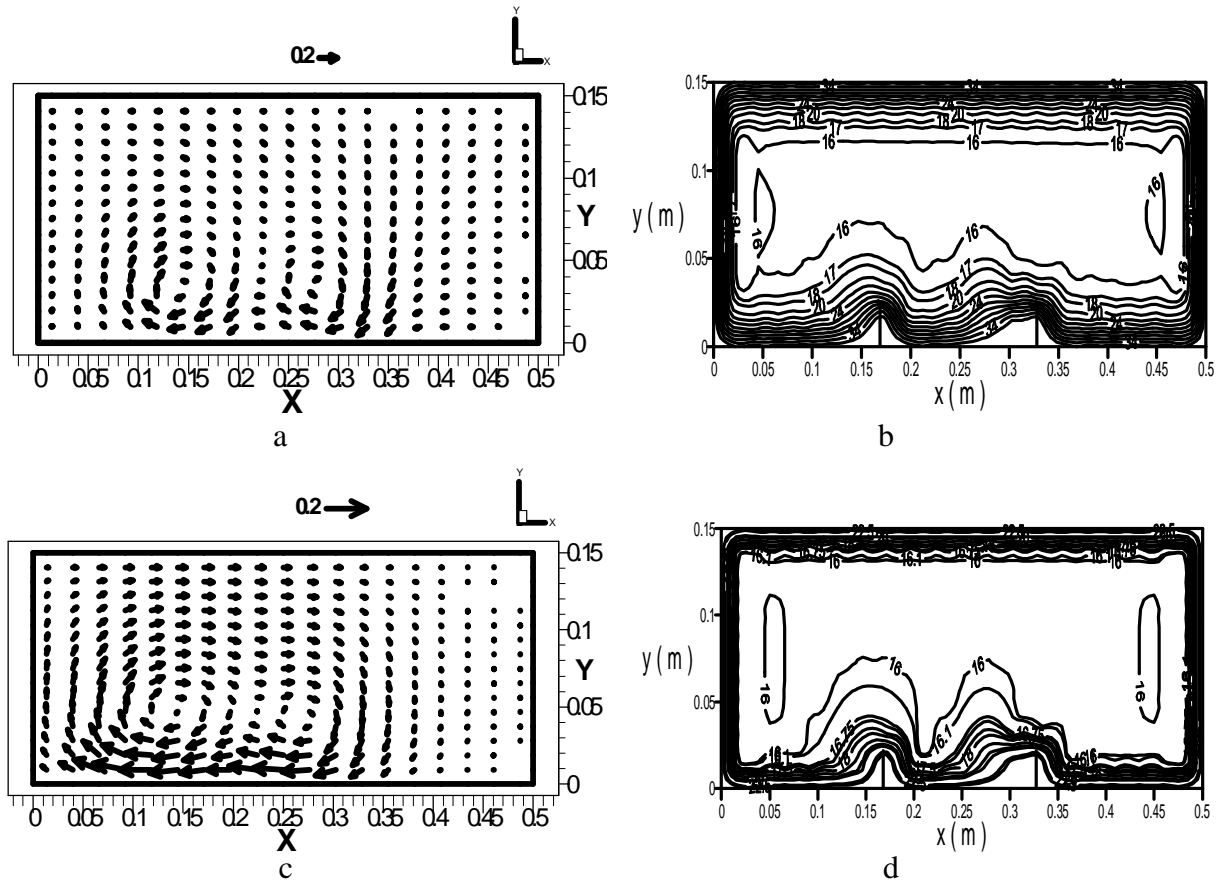
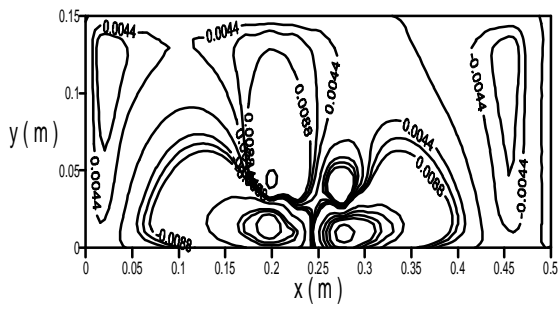
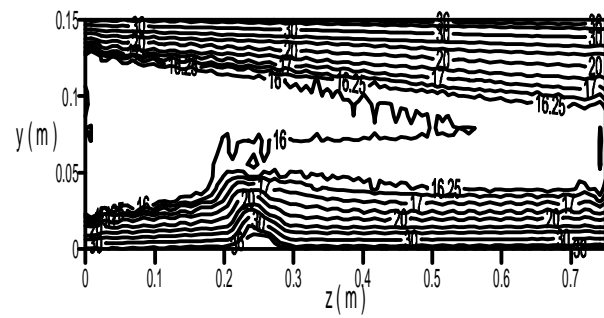


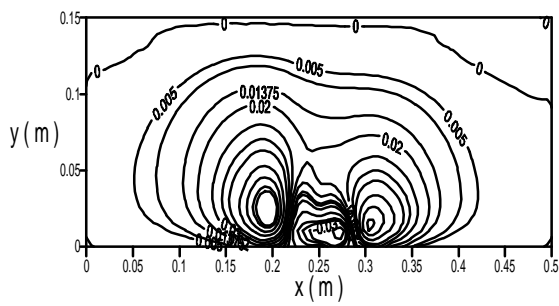
Fig.(9) Velocity vectors and temperature contours for duct flow with winglet pair in (x-y) plane: (a) Velocity vectors for laminar flow, (b) Temperature contours where ($T_{wall}=40C^{\circ}$ & $T_{in}=16C^{\circ}$) for laminar flow, (c) Velocity vectors for turbulent flow, and (d) Temperature contours where ($T_{wall}=25C^{\circ}$ & $T_{in}=16C^{\circ}$) for turbulent flow.



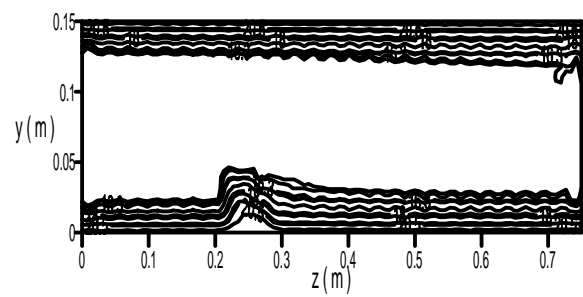
a



b



c



d

Fig.(10) Velocities and temperatures contours for duct flow with rectangular VG (represented in figure (1-b): (a) u / w_{in} in (x-y) plane for laminar flow, (b) T in (z-y) plane for laminar flow, (c) v / w_{in} in (x-y) plane for turbulent flow, and (d) T in (z-y) plane for turbulent flow.

References

1. F. Durst, M. Founti, and S. Obi, "Experimental and computational investigation of the two-dimensional channel flow over two fences in tandem", transaction of the ASME, journal of fluid engineering, March 1988, vol. 110, pp.48-54.
2. K. Ichimiya, "Effects of several roughness elements on an insulated wall for heat transfer from opposite smooth heated surface in a parallel plate duct", transactions of the ASME, journal of heat transfer, February 1987, Vol. 109, PP. 68-73
3. Hajime Yokosawa, Hideomi Fujito, Masafumi Hirota, and Shotaro Iwata, "Measurement of turbulent flow in a square duct with a roughened walls on two opposite sides", Int. J. heat and fluid flow, Vol. 10, No. 2, June 0989, PP.125-130.
4. C. -O. Olsson and B. Sunden, "Thermal and hydraulic performance of a rectangular duct with multiple V-Shaped ribs", transactions of ASME, journal of heat transfer, November 1998, Vol.120, PP.1072-1077.
5. M. Fiebig, u. Brockmeier, N.K. Mitra, and T. Güntermann, "STRUCTURE OF VELOCITY AND TEMPERATURE FIELDS IN LAMINAR CHANNEL FLOWS WITH LONGITUDINAL VORTEX GENERATORS", Numerical heat transfer, part A, vol. 15, PP.281-302, 1989.
6. A.Y. Turk and G.H. Junkhan, "Heat transfer enhancement downstream of vortex generators on a flat plate", proceeding of the Eighth international heat transfer conference, Vol. 6, PP.2903-2908.
7. TR FODEMSKI and MW COLLINS, "Flow and heat transfer simulations for two-and three-dimensional smooth and ribbed channels", Second UK National conference on heat transfer, C134/88, PP.845-860.
8. J.C. HAN, "Heat transfer and friction characteristics in rectangular channels with rib turbulators", Transactions of the ASME, journal of the heat transfer, May 1988, Vol. 110, PP. 321-328.
9. M.J. Lewis, "An elementary analysis for predicting the momentum-and heat-transfer characteristics of a hydraulically rough surface", Transactions of ASME, journal of heat transfer, May 1975, PP. 249-254.
10. Chin-Hsiang Cheng and Wen-Hsiung Huang, "LAMINAR FORCED CONVECTION FLOWS IN HORIZONTAL CHANNELS WITH TRANSVERSE FINS PLACED IN INTRANCE REGIONS", Numerical heat transfer, part A, Vol. 16, PP. 77-100, 1989.D.E. Metzger, R.A. Berry, and J.P. Bronson, "Developed heat transfer in rectangular ducts with staggered arrays of short pin fins", transactions of the ASME, Journal of heat transfer, November 1982, Vol. 104, PP.700-706.
11. S.C.Lau, J.C. Han, and T.Batten, "Heat Transfer, Pressure Drop, and Mass Flow Rate in Pin Fin Channels With Long and Short Trailing Edge Ejection Holes", transactions of the ASME, Journal of heat transfer, April 1989, Vol. 111, PP.116-123.
12. W.S.MOHAMMAD,"Space Air-Conditioning of Mechanically Ventilated Rooms: Computation of Flow and Heat Transfer", Ph.D. thesis, Cranfield Institute of Technology, School of Mechanical Engineering, June 1986.
13. Sattar J.H., "Experimental and Computational Study of Three Dimensional Turbulent Mixed Convection for Cooling of Electronic Components in Enclosure", Ph.D.Thesis, University of Technology, Mechanical ENG.DEP, July 2003.
14. Sabah Tarik Ahmed,"Numerical & Experimental Study on Heat Transfer Enhancement by Vortex Generator", Ph.D.Thesis, University of Technology, Mechanical ENG. DEP., September 2001.
15. G.BISWAS and H.CHATTOPADHYAY, "Heat transfer in a channel with built-in wing-type vortex generators", Int. J. Heat Mass Transfer, Vol.35, No.4, pp.803-814, 1992.